IOPscience iopscience.iop.org

Home Search Collections Journals About Contact us My IOPscience

The persistance of strain in dynamical systems

This article has been downloaded from IOPscience. Please scroll down to see the full text article.

1989 J. Phys. A: Math. Gen. 22 971

(http://iopscience.iop.org/0305-4470/22/8/013)

View the table of contents for this issue, or go to the journal homepage for more

Download details:
IP Address: 129.252.86.83
The article was downloaded on 31/05/2010 at 13:55

Please note that terms and conditions apply.

J. Phys. A: Math. Gen. **22** (1989) 971-984. Printed in the UK

The persistence of strain in dynamical systems

E Dresselhaus and M Tabor

Department of Applied Physics, Columbia University, New York, NY 10027, USA

Received 24 August 1988, in final form 14 November 1988

Abstract. A dynamical exponent, termed the 'persistence of strain', is defined for systems of ordinary differential equations. Analogy with fluid dynamics suggests that it can provide a convenient—and easily computed—characterisation of a dynamical system and, in particular, the geometry of attracting sets.

1. Introduction

In this paper we suggest that a certain dynamical quantity, termed the 'persistence of strain', which has specific fluid mechanical applications, can also provide a useful geometrical characterisation of dynamical systems in general. The motivation for this idea is the much studied problem in polymer physics of polymer extension in a four (or more) roll mill (see, for example, Berry and Mackley 1977). Here, the two-dimensional velocity fields provided by this type of apparatus are of the 'persistently extensional' type required to obtain significant molecular stretching (Frank and Mackley 1976). Frank (see Berry and Mackley 1977, Frank and Mackley 1976) has suggested that these velocity fields are conveniently characterised by a quantity, the 'persistence of strain', which is defined as follows. For a two-dimensional incompressible velocity field the velocity components can be defined in the usual way through a stream function $\psi = \psi(\boldsymbol{x}, t)$ (where $\boldsymbol{x} = (x, y)$), namely

$$u = \psi_y \qquad v = -\psi_x. \tag{1.1}$$

The vorticity is

$$\omega = \tfrac{1}{2}(v_x - u_y) = -\tfrac{1}{2}\nabla^2\psi \tag{1.2}$$

and the strain rate tensor is

$$S = \begin{pmatrix} u_x & \tfrac{1}{2}(u_y + v_x) \\ \tfrac{1}{2}(u_y + v_x) & v_y \end{pmatrix} = \begin{pmatrix} \psi_{xy} & \tfrac{1}{2}(\psi_{yy} - \psi_{xx}) \\ \tfrac{1}{2}(\psi_{yy} - \psi_{xx}) & -\psi_{xy} \end{pmatrix}. \tag{1.3}$$

The principal rate of strain s is defined by

$$s^2 = -\det S = \tfrac{1}{4}(\psi_{yy} - \psi_{xx})^2 + \psi_{xy}^2. \tag{1.4}$$

Using (1.2) and (1.3) the *persistence of strain* is now defined as

$$\sigma(\boldsymbol{x}, t) = (s^2 - \omega^2)^{1/2} = (-K(\psi))^{1/2} \tag{1.5}$$

where $K(\psi)$ is the determinant of the second derivative of ψ, namely

$$K(\psi) = \psi_{xx}\psi_{yy} - \psi_{xy}^2. \tag{1.6}$$

0305-4470/89/080971+14$02.50 © 1989 IOP Publishing Ltd

$K(\psi)$ can be thought of as an 'unnormalised' Gaussian curvature: it does reflect the curvature of fluid trajectories but cannot, for example, detect the difference in shape between two circular trajectories of radius ρ and ρ' with $\rho > \rho'$. (The normalised curvatures are $1/\rho$ and $1/\rho'$, respectively—the unnormalised curvature (1.6) is a constant for both cases.) Clearly σ is only real when the unnormalised curvature of ψ is negative. It is precisely in this situation that the flow field is (locally) hyperbolic, thereby leading to exponential stretching of a fluid element and hence the possibility of significant polymer extension. If the flow is vorticity dominated, i.e. $\omega^2 > s^2$, σ becomes imaginary and a fluid element will (locally) 'tumble' rather than 'stretch'. We also note that it is often convenient to consider the squared persistence of strain as well, i.e.

$$\sigma^2(x, t) = s^2 - \omega^2. \tag{1.7}$$

2. Persistence of strain in three dimensions

The definition of σ^2 in terms of the unnormalised Gaussian curvature of the stream function is specific to two-dimensional problems and a natural question to ask is: how might such a quantity be (uniquely) defined for three-dimensional velocity fields or, for that matter, flow fields of any dimension? For now we concentrate on the physical problem of 3D fluids and propose that the desired quantity is simply

$$\sigma^2(x, t) = \tfrac{1}{2} \operatorname{Tr} A^2 \tag{2.1}$$

where A is the velocity deformation tensor, i.e.

$$A_{ij} = \partial_j u_i \qquad i, j = 1, 2, 3. \tag{2.2}$$

If S is the symmetric (strain rate tensor) and Ω the antisymmetric (vorticity tensor) parts of A, respectively, i.e.

$$S_{ij} = \tfrac{1}{2}(A_{ij} + A_{ji}) \qquad \Omega_{ij} = \tfrac{1}{2}(A_{ij} - A_{ji}) \tag{2.3}$$

then

$$\sigma^2(x, t) = \tfrac{1}{2} \operatorname{Tr} (S + \Omega)^2 = \tfrac{1}{2}(\operatorname{Tr} S^2 + \operatorname{Tr} \Omega^2) \tag{2.4}$$

where we have used the fact that antisymmetric tensors (the products $S\Omega$ and ΩS) have zero trace. In two dimensions the definition of σ^2, (2.1), is easily verified to be identical to the original definition (1.7).

The tensor S has real eigenvalues s_i and orthonormal eigenvectors $\boldsymbol{\xi}_i$, so that $\operatorname{Tr} S^2 = \Sigma_i s_i^2$. (Here $\boldsymbol{\xi}_i$ are the principal directions of shear and s_i are the associated principal shears.) Since $\operatorname{Tr} \Omega^2 = -\Sigma_i \omega_i^2$, where $\boldsymbol{\omega} = \frac{1}{2}\nabla \times \boldsymbol{u}$ is the vorticity, the persistence of strain can be written as

$$\sigma^2(x, t) = \tfrac{1}{2} \sum_{i=1}^{N} s_i^2(x, t) - \omega_i^2(x, t) \qquad N = 2, 3, \ldots. \tag{2.5}$$

In this light σ^2 measures the balance between shear-dominated and vorticity-dominated flow about the point x. If $\sigma^2 < 0$ the flow is vorticity dominated; if $\sigma^2 > 0$ the flow is shear dominated. Note that $\operatorname{Tr} A = 0$, so the principal shears s_i and directions $\boldsymbol{\xi}_i$ are not mutually independent. In planar flow, we have only one shear and one vorticity, and the persistence of strain tells us exactly which of shear or vorticity dominates the

flow. The situation is different in three dimensions, where we have three components of shear and vorticity. Now we can have shear domination in one principal direction and vorticity domination about another. Thus, the persistence of strain in three dimensions gives a little less information about the exact nature of the local fluid flow than in two dimensions.

The quantity σ^2 enjoys a number of nice physical properties. For example, if we have an incompressible viscous fluid in a two- or three-dimensional domain V, then

$$\int_V \mathrm{d}\boldsymbol{x}\, \sigma^2(\boldsymbol{x}, t) = 0. \tag{2.6}$$

To see this we write

$$\begin{aligned}\sigma^2(\boldsymbol{x}, t) &= \sum_{i,j} (\partial_i u_j) \cdot (\partial_j u_i) \\ &= \sum_{i,j} \partial_i (u_j \partial_j u_i) - u_j \partial_j \partial_i u_i \\ &= \nabla \cdot (\boldsymbol{u} \cdot \nabla)\boldsymbol{u}\end{aligned}$$

where we have used the Leibnitz rule in the second line and the incompressibility condition $\partial_i u_i = 0$ in the third. Then, if $\hat{n}(\boldsymbol{x})$ is the outward unit normal on ∂V:

$$\int_V \mathrm{d}\boldsymbol{x}\, \sigma^2(\boldsymbol{x}, t) = \int_{\partial V} \hat{n} \cdot (\boldsymbol{u} \cdot \nabla)\boldsymbol{u}\, \mathrm{d}a = 0 \tag{2.7}$$

since $\boldsymbol{u}|_{\partial V} = 0$ for solutions to the Navier–Stokes equations. Note that if viscosity is not present we have Euler's equations and $\hat{n} \cdot \boldsymbol{u}|_{\partial V} = 0$. Thus

$$\int_V \mathrm{d}\boldsymbol{x}\, \sigma^2(\boldsymbol{x}, t) = \int_{\partial V} \sum_{i,j} u_i u_j\, \partial_i n_j \equiv \kappa(t) \tag{2.8}$$

is non-zero unless the walls of the domain have everywhere zero curvature, as $\partial_i n_j$ is just the curvature tensor. If the boundary conditions have no explicit time dependence then κ is constant, and equation (2.8) is independent of time. $\kappa(t)$ in some sense measures the total amount of curvature of the fluid trajectories (normalised by a squared velocity) at the boundary of the vessel V at a time t. For both viscous and non-viscous steady flows equations (2.6) and (2.8) express 'conservation laws'. These conservation laws make intuitive sense if we imagine circularly stirring a fluid in a small neighbourhood of a point $\boldsymbol{x}_0$. The stirring will cause local vorticity domination ($\sigma^2 < 0$). Equations (2.6) and (2.8) mathematically express the fact that some shear must be produced in the vicinity of $\boldsymbol{x}_0$ to balance the increased vorticity at $\boldsymbol{x}_0$.

The persistence of strain is a very simple quantity to calculate. Given a velocity field, Tr A^2 is a trivial calculation and later we will show that it can also give non-trivial information about the dynamics of any ODE. If we are not given an explicit velocity field (as in almost all fluid mechanics applications), the persistence of strain is still reasonably easy to calculate. Finite-difference-style numerical computations of the Navier–Stokes equation invariably progress by guessing a pressure $p(\boldsymbol{x}, t)$ and using the derived velocity fields to refine the guessed pressure via

$$\nabla \cdot (\boldsymbol{u} \cdot \nabla)\boldsymbol{u} = -\nabla^2 p/\rho \equiv \sigma^2. \tag{2.9}$$

Since the left-hand side is known, this is just the Poisson equation for $p(\boldsymbol{x}, t)$. This process is iterated and, hopefully, converges to a solution. The persistence of strain

can be calculated without additional effort. In contrast, most other combinations of derivatives A_{ij} would require some numerical differentiation and increased round-off error. Spectral methods are the other major numerical tool for solving the fluid equations. Here, we use Fourier transforms to find an approximate solution to the two-dimensional vorticity equation

$$\partial \boldsymbol{\omega}/\partial t = -(\boldsymbol{u} \cdot \nabla)\boldsymbol{\omega} + \nu \nabla^2 \boldsymbol{\omega}. \tag{2.10}$$

As in the case of finite-difference algorithms, we can easily calculate the persistence of strain. In two dimensions, after the stream function ψ is obtained from $\boldsymbol{\omega}(\boldsymbol{x}, t)$ by inverting

$$-\nabla^2 \psi(\boldsymbol{x}, t) = \boldsymbol{\omega}(\boldsymbol{x}, t) \tag{2.11}$$

in Fourier space, we use (1.5) to calculate σ^2. Evaluating the Gaussian curvature of ψ is a simple matter in Fourier space. A similar method can be employed in the three-dimensional case. Overall the persistence of strain is as easily computed as other fluid dynamical quantities.

So far we have only considered the persistence of strain in the Eulerian description, i.e. as a function of position, $\boldsymbol{x}$, in the fixed coordinate frame of the fluid. It is, however, ideally suited for computation in the *Lagrangian* description, i.e. following individual fluid particle trajectories. For a given velocity field, $\boldsymbol{u}$, the fluid particles satisfy the ordinary differential equations

$$\begin{aligned} \dot{x}_1 &= u_1(\boldsymbol{x}, t) \\ \dot{x}_2 &= u_2(\boldsymbol{x}, t) \\ \dot{x}_3 &= u_3(\boldsymbol{x}, t) \end{aligned} \tag{2.12}$$

and the local variations δx_i satisfy

$$\frac{\mathrm{d}}{\mathrm{d}t}\begin{pmatrix} \delta x_1 \\ \delta x_2 \\ \delta x_3 \end{pmatrix} = A \begin{pmatrix} \delta x_1 \\ \delta x_2 \\ \delta x_3 \end{pmatrix} \tag{2.13}$$

where A is, of course, just the velocity deformation tensor defined in (2.2). In the language of dynamical systems (2.13) is just the tangent map of the flow (2.12). For a given initial condition, $\boldsymbol{x}_0$, we can follow the persistence of strain along a fluid particle orbit and we call $\sigma^2 = \sigma^2(\boldsymbol{x}_0, t)$ the *strain history* of that particle. Even very simple velocity fields can generate chaotic fluid particle trajectories (see, for example, Aref 1983, Chaiken *et al* 1986) and we can expect $\sigma^2(\boldsymbol{x}_0, t)$ to exhibit highly complex behaviour.

For such trajectories we expect the strain history to oscillate wildly between shear domination and vorticity domination. This being so, it will be useful to calculate the power spectral density of σ^2:

$$P(\boldsymbol{x}_0, f) = |\tilde{\sigma}^2(\boldsymbol{x}_0, f)|^2 \tag{2.14}$$

where

$$\tilde{\sigma}^2(\boldsymbol{x}_0, f) = \int_{-\infty}^{+\infty} \mathrm{d}t \exp(2\pi \mathrm{i} f t)\sigma^2(\boldsymbol{x}_0, t). \tag{2.15}$$

The Fourier representation gives us a good measure of the complexity of the flow. We expect that strains along chaotic trajectories will have very many significantly strong

modes in their power spectra, whereas power spectra of strains along regular trajectories will have but a few δ-function-like peaks.

Another related quantity is the persistence of strain autocorrelation function:

$$C(\boldsymbol{x}_0, \tau) = \langle \sigma^2(\boldsymbol{x}_0, t)\sigma^2(\boldsymbol{x}_0, t+\tau)\rangle = \lim_{T\to\infty} \frac{1}{T}\int_{-T}^{+T} \mathrm{d}t\, \sigma^2(\boldsymbol{x}_0, t)\sigma^2(\boldsymbol{x}_0, t+\tau). \tag{2.16}$$

$C(\boldsymbol{x}_0, \tau)$ is the Fourier transform of the power spectrum $P(\boldsymbol{x}_0, f)$ (via the Wiener-Khinchin theorem), so we are really just looking at the same information in a different way. For periodic motions $C(\boldsymbol{x}_0, \tau)$ will be periodic, and particle motions will remain well correlated for long times. For chaotic motions, we should expect that $C(\boldsymbol{x}_0, \tau)$ falls off fairly rapidly, signifying that, after a fairly short time, particles completely lose memory of their past straining activity. (As an aside, we mention that we believe this correlation function to be the key quantity for studying the dynamics of polymers in turbulent flows. Understanding this process is crucial in a variety of problems including, particularly, that of drag reduction (see Tabor and de Gennes (1986).) It will also be of use to compare the Lagrangian correlation function (2.16) with its Eulerian counterpart, namely

$$C'(\boldsymbol{\xi}, t) = \langle \sigma^2(\boldsymbol{x}, t)\sigma^2(\boldsymbol{x}+\boldsymbol{\xi}, t)\rangle = \frac{1}{\mathrm{vol}(V)}\int_V \mathrm{d}\boldsymbol{x}\, \sigma^2(\boldsymbol{x}, t)\sigma^2(\boldsymbol{x}+\boldsymbol{\xi}, t) \tag{2.17}$$

to extract characteristic length scales for the fluid flow.

3. Numerical experiment: the ABC flows

Here we illustrate numerically some of the ideas above. The Arnold-Beltrami-Childress (ABC) flows, generated from the velocity field

$$\boldsymbol{u}(\boldsymbol{x}) = (A\sin z + C\cos y,\ B\sin x + A\cos z,\ C\sin y + B\cos x) \tag{3.1}$$

are steady-state solutions to Euler's equation which exhibit a great variety of complex Lagrangian behaviour (see Dombre *et al* 1986). Figure 1, a Poincaré plot of intersections with the $z = 0$ plane for $A = 1$, $B = 1/\sqrt{2}$, $C = 1/\sqrt{3}$ (throughout we will consider only these parameter values), shows periodic orbits (to the left), a single chaotic trajectory (filling much of the right) and KAM surfaces breaking up (the island structures to the right amid the chaotic trajectory). It may be reasonable to anticipate that the ABC flows display Lagrangian behaviour that is, in some sense, typical of chaotic fluid flow, since many numerical schemes for solving the fluid equations use spectral expansions resulting in a Fourier expansion for the velocity fields (the ABC flow is itself a simple combination of trigonometric functions). True justification for this remark must, however, await the further investigation of real (numerical) solutions to the Navier-Stokes equation. In any case, the ABC flows are much more convenient to study than real flows, because of the simple analytic form of the velocity field.

For the ABC flows the persistence of strain takes the simple form:

$$\sigma^2(x, y, z) = -(BC\cos x \sin y + AB\sin x\cos z + AC\cos y\sin z). \tag{3.2}$$

Throughout these studies we take $\boldsymbol{x}_{\text{chaotic}} = (0, 0, 0)$ and $\boldsymbol{x}_{\text{chaotic}} = (\pi, \pi, 0)$ as initial conditions generating typical chaotic trajectories; we also take $\boldsymbol{x}_{\text{periodic}} = (1, 0, 0)$ as generating a typical periodic trajectory. The quantities of interest (spectral densities

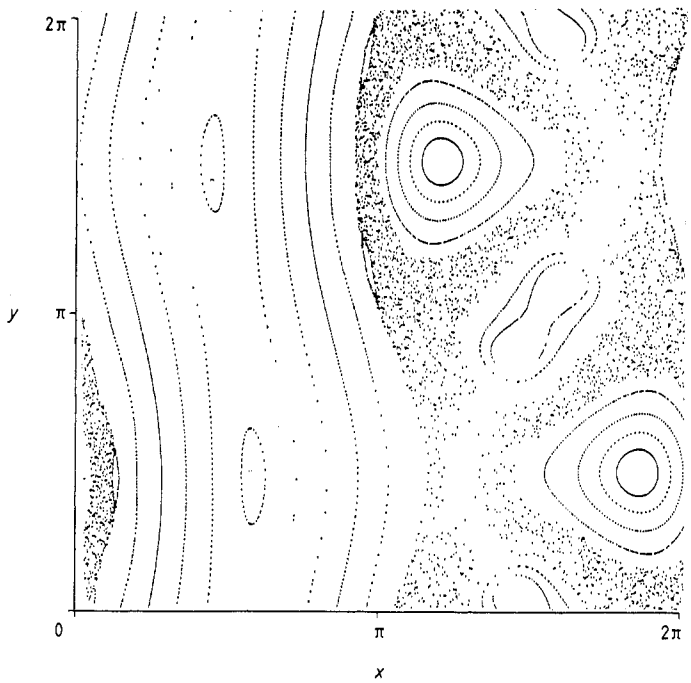

Figure 1. Poincaré plot of intersections with the $z = 0$ plane for $A = 1$, $B = 1/\sqrt{2}$, $C = 1/\sqrt{3}$ (after Dombre *et al* 1986).

and autocorrelations) are qualitatively unchanged for both of these different choices of chaotic trajectory, as well as for initial conditions randomly chosen in some small ball about a chaotic one. Figures 2(a) and (b) contrast $\sigma^2(\boldsymbol{x}_0, t)$ for chaotic and periodic trajectories, respectively, and point to the necessity of using spectral quantities to unravel the wild oscillations of σ^2 for a chaotic trajectory. Figure 3 shows the average power spectrum $\bar{P}(f)$ for a chaotic trajectory. Averaging is performed over ten randomly chosen initial conditions in a ball of distance 0.1 units about $\boldsymbol{x}_{\text{chaotic}}$. The envelope lineshape of $\bar{P}(f)$ is quite insensitive to averaging or to the choice of (chaotic) initial condition. Averaging over different sets of these initial conditions changes only a few details of the power spectrum, and not its overall lineshape. The peaked nature of these spectra indicate that we could very crudely approximate $\sigma^2(t) \approx \cos(f_0 t)$, where f_0 is the frequency at which the peak occurs. This approximation gives us a rough timescale, $T_0 = 1/f_0$, at which particles jump from 'eddy' to 'eddy' (defined here as areas where $\sigma^2 < 0$). Power spectra of position and velocity for typical chaotic trajectories, shown in figures 4(a) and (b), decay exponentially as a function of frequency and have a fundamentally different shape from the power spectra of σ^2. (This is not surprising since σ^2, a derivative of $\boldsymbol{u}$, has an entirely different physical interpretation.) Figure 5 shows the persistence of strain autocorrelation function, for typical chaotic trajectories, which decays rapidly to a regular oscillatory behaviour which persists even at the longest time lags. For comparison purposes we show in figures 6(a) and (b) the autocorrelation functions of position and velocity, respectively. These autocorrelations exhibit the expected initial exponential fall-off typical of chaotic orbits. However, the long-time oscillations of these autocorrelation functions appear to be far less regular than those found for the persistence of strain autocorrelation.

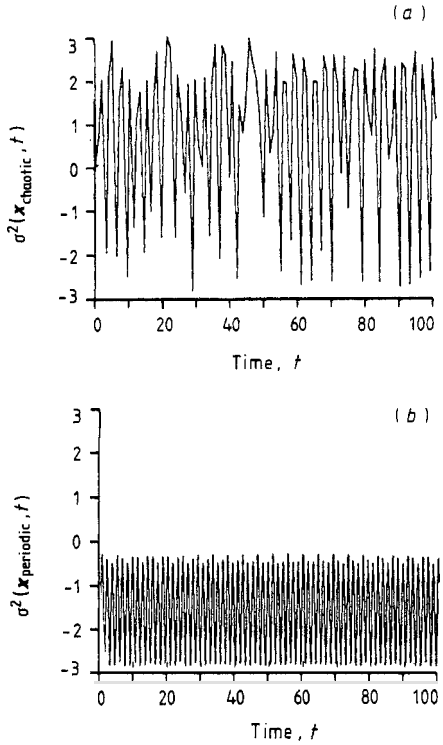

Figure 2. $\sigma^2(x_0, t)$ for (a) typical chaotic and (b) periodic trajectories.

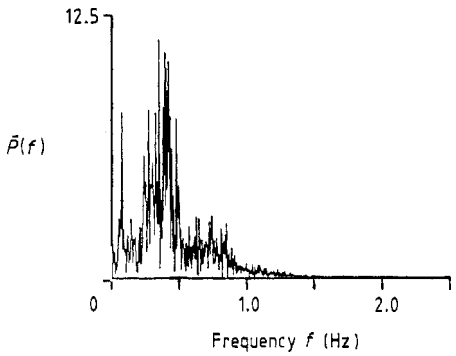

Figure 3. Power spectrum $\bar{P}(f)$ of the persistence of strain averaged over close chaotic initial conditions.

4. Persistence of strain as a dynamical exponent

Although the persistence of strain has a natural fluid dynamical context we now suggest that it can be a useful—and very easily computed—quantity for characterising dynamical systems. Any motion governed by the system of ODE:

$$\mathrm{d}x/\mathrm{d}t = u(x, t) \qquad x(0) = x_0 \tag{4.1}$$

are locally characterised by some combination of stretching and folding components.

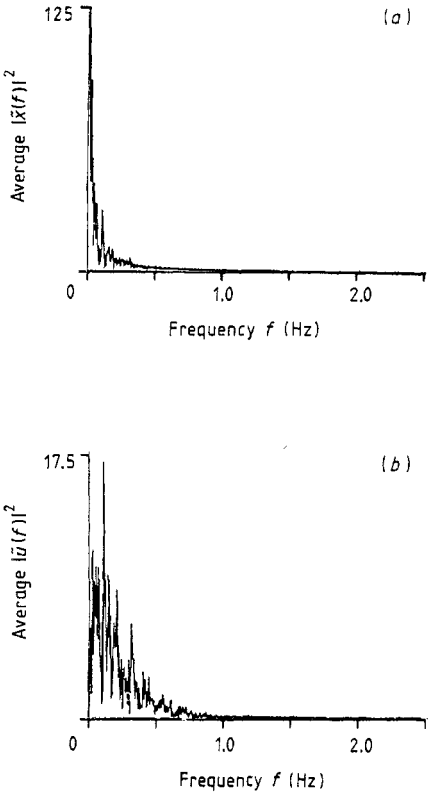

Figure 4. Power spectra of (a) position $x(t)$ and (b) velocity $u(t)$ averaged over close chaotic initial conditions.

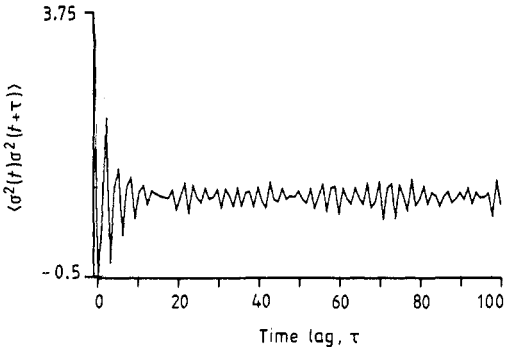

Figure 5. Typical persistence of strain autocorrelation $\langle\sigma(t)\sigma^2(t+\tau)\rangle$ for a single chaotic trajectory.

Stretching, whether expansive or contractive, comes from the real parts of the eigenvalues of the tangent map matrix

$$A(\boldsymbol{x}_0, t) = D\boldsymbol{u}_{\boldsymbol{x}_0} \qquad A_{ij} = \partial_j u_i \qquad i, j = 1, \ldots, N \tag{4.2}$$

and folding from the imaginary parts of these eigenvalues.

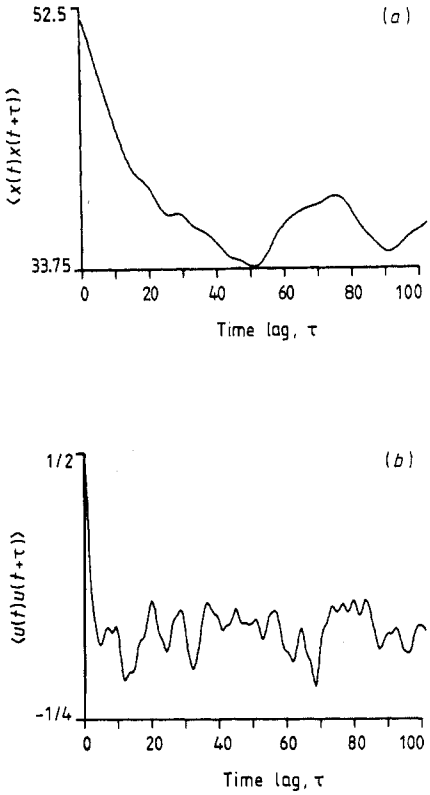

Figure 6. Typical position and velocity autocorrelations: (*a*) $\langle x(t)x(t+\tau)\rangle$ and (*b*) $\langle u(t)u(t+\tau)\rangle$.

If we are interested in characterising the balance between the stretching and folding actions of a dynamical system in terms of a *single* number (or 'exponent') we are naturally led to consider either determinants, $\det A^n$, or traces, $\mathrm{Tr}\, A^n$. In the case of determinants the relationship $\det A^n = (\det A)^n$ cuts down the useful determinantal quantities to just $\det A$ itself. Furthermore, if the eigenvalues of A are complex conjugate pairs $\lambda_i = \alpha_i + \mathrm{i}\beta_i$, then

$$\det A = \prod_{j=1}^{N} (\alpha_j^2 + \beta_j^2)$$

in which case the contribution of real and imaginary parts cannot be separated out. Turning to trace quantities, the first trace, $\mathrm{Tr}\, A = \Sigma_{j=1}^{N} \lambda_j$, has the disadvantage that all the imaginary parts of the complex conjugate λ_j will cancel out. Clearly the natural quantity is the second trace, namely

$$\mathrm{Tr}\, A^2 = \sum_{j=1}^{N} \lambda_j^2 = \sum_{j=1}^{N} (\alpha_j^2 - \beta_j^2). \tag{4.3}$$

Evidently the sign and magnitude of $\mathrm{Tr}\, A^2$ measures the balance between stretching and folding. In principle, one could also consider higher traces, i.e. $\mathrm{Tr}\, A^n$, $n \geqslant 3$, but these quantities will involve complicated combinations of the α_j and β_j that are difficult to interpret. The persistence of strain quantity (4.3) is clearly far easier to compute

along a system orbit than, say, the Lyapunov exponents and may indeed contain additional information since the latter quantity is, in effect, only concerned with the real parts of the eigenvalues.

A simple way of gleaning global information from the persistence of strain is by averaging. Averaging the persistence of strain over a trajectory (or any flow-invariant set, for that matter) can give some notion of whether the set is dominated by stretching or folding. One problem is immediately apparent with averaging σ^2 in this way. The regions of stretch ($\sigma^2>0$) and fold ($\sigma^2<0$) when summed up will cancel in some complicated fashion. It is far more (physically) useful if we can separate these two types of region. This can be neatly accomplished with

$$\bar{\sigma}(I)=\frac{1}{\mathrm{vol}(I)}\int_I \mathrm{d}x[\sigma^2(x,t)]^{1/2}=\bar{\sigma}_{\mathrm{Re}}(I)+\mathrm{i}\bar{\sigma}_{\mathrm{Im}}(I) \tag{4.4}$$

where I is some flow-invariant set (whether trajectory, limit cycle, attractor, etc). The square root nicely separates stretch from fold as the real and imaginary averages $\bar{\sigma}_{\mathrm{Re}}$ and $\bar{\sigma}_{\mathrm{Im}}$. To summarise this information it is useful to measure the ratio of stretch to fold, namely the quantity

$$\chi=\bar{\sigma}_{\mathrm{Re}}/\bar{\sigma}_{\mathrm{Im}}. \tag{4.5}$$

It is interesting to note that χ is, in effect, the inverse of the so-called kinematical vorticity number proposed many years ago by Truesdell (1954). There, in a strictly fluid dynamical context, it was conjectured that a large value of this number would characterise a strongly turbulent flow field.

The two numbers $\bar{\sigma}_{\mathrm{Re}}(I)$ and $\bar{\sigma}_{\mathrm{Im}}(I)$ give significant information about the shape of the invariant set I. The bifurcation of the Van der Pol equation:

$$\begin{aligned}\dot{x}&=y+x(\mu-x^2)\\ \dot{y}&=-x\\ \sigma^2(x,y)&=\tfrac{1}{2}(\mu-3x^2)^2-1\end{aligned} \tag{4.6}$$

as the parameter μ goes from -1 through 0 to 1, gives a nice illustration of how these quantities can be used to characterise an attractor. Figure 7 shows how this bifurcation is characterised by the average persistence of strain. Comparison of figure 7(a) with (b) and (c) clearly shows how skewness of the limit cycle, increasing with positive μ, is expressed by the number $\chi(\mu)$.

Along these lines, figure 8 shows how a trajectory of the ABC flows ($x_{\mathrm{chaotic}}=(0,0,0)$) makes the transition from regular (for $C=0$) to chaotic behaviour (for $C=1/\sqrt{3}$). This sharp rise in χ seems to be typical of the transition to chaotic dynamics.

Figures 9 shows the Lorenz system:

$$\begin{aligned}\dot{x}&=\rho(y-x)\\ \dot{y}&=Rx-y-xz\\ \dot{z}&=xy-bz\\ \sigma^2(x,y,z)&=\tfrac{1}{2}(\rho^2+b^2+1)+\rho(R-z)-x^2\end{aligned} \tag{4.7}$$

for $\rho=10$, $b=\frac{8}{3}$ and the Rayleigh number $20\leqslant R\leqslant 200$. The persistence of strain average $\bar{\sigma}$ is averaged over five randomly chosen initial conditions. We can see the sudden rise in χ, corresponding to the appearance of a strange attractor at $R\approx 24.7$, the gradual fall in χ, corresponding to the collapse to a limit cycle at $R\approx 150$, and the less violent, but still marked, rise corresponding to the second attractor at $R\approx 166$. It

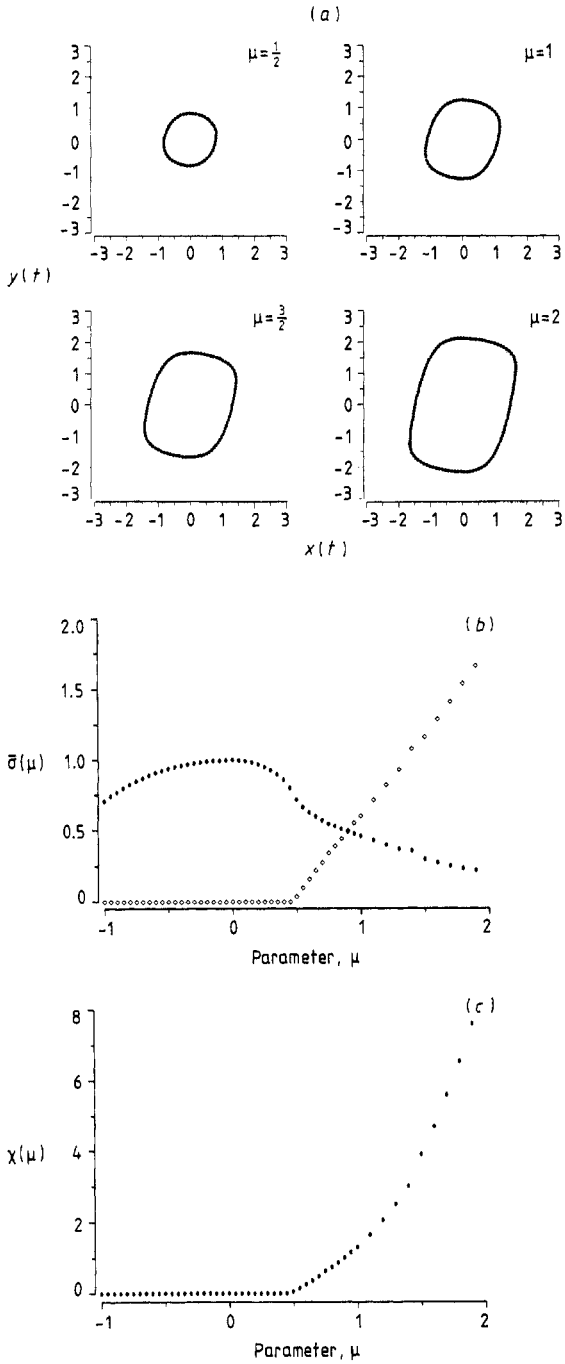

Figure 7. The Van der Pol limit cycle as an example of how χ can be used to characterise the geometry of an attracting set. (a) shows the shape of the limit cycle for $\mu = \frac{1}{2}$, $\mu = 1$, $\mu = \frac{3}{2}$ and $\mu = 2$. (b) and (c) show how primarily circular motion (for $\mu > 0$) becomes increasingly distorted as μ increases, and how these changes in geometry are illustrated by the quantities $\bar{\sigma}(\mu)$ and $\chi(\mu)$, respectively. In (b) $\diamond$ plots $\bar{\sigma}_{\mathrm{Re}}$ and $\bullet$ plots $\bar{\sigma}_{\mathrm{im}}$.

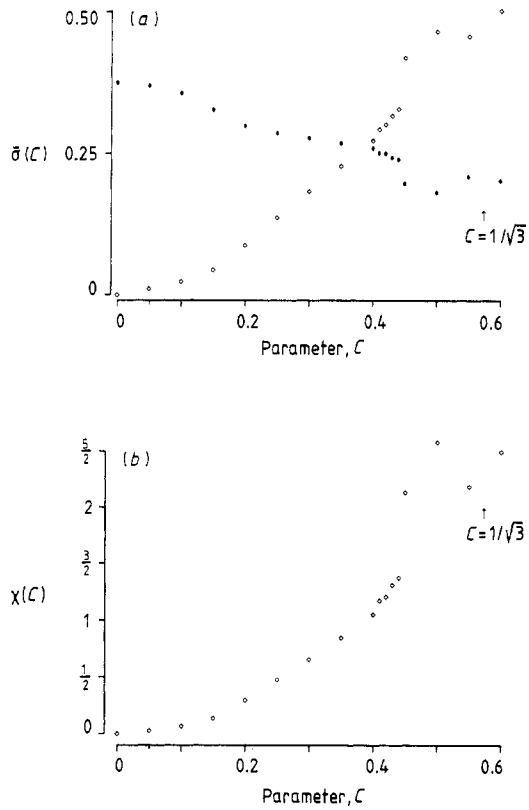

Figure 8. (*a*) $\bar{\sigma}(C)$ plotted against C and (*b*) $\chi(C)$ plotted against C for the ABC flows with $A=1$, $B=1/\sqrt{2}$, and C in the range $0 \leqslant C \leqslant 0.6$, passing through $C=1/\sqrt{3}$, the canonical chaotic regime. Averaging was performed over the chaotic trajectory $x_{\text{chaotic}} = (0, 0, 0)$ for 3000 time units. The largest error here is for $\chi(\frac{1}{2}) = 2.57 \pm 0.01$. In (*a*) $\diamond$ plots $\bar{\sigma}_{\text{Re}}$ and $\bullet$ plots $\bar{\sigma}_{\text{Im}}$.

is unclear why this second attractor exhibits a less marked increase in χ than the one at $R \approx 24.7$.

Figure 10 shows the period-doubling transition from regular to chaotic motion in the Rössler system:

$$\begin{aligned} \dot{x} &= -(y+z) \\ \dot{y} &= x+0.2y \\ \dot{z} &= 0.2+xz-Cz \\ \sigma^2(x, y, z) &= \tfrac{1}{2}(x-C)^2 - z - 0.98. \end{aligned} \tag{4.8}$$

Again we have averaged over five random initial conditions. We note that the Rössler attractor (in its chaotic regime) is much more heavily dominated by stretching motions than the Lorenz attractor. The Rössler attractor attains a value of χ over 30, whereas the Lorenz attractor only reaches about 1.5.

The ragged bumps in these figures arise from numerical errors. It seems to be quite difficult to make these averages converge to any desired accuracy. The errors reported in the figures have been calculated by averaging the persistence of strain for an extra time (quite large relative to the total time of averaging), and measuring the difference between this longer average and the original one.

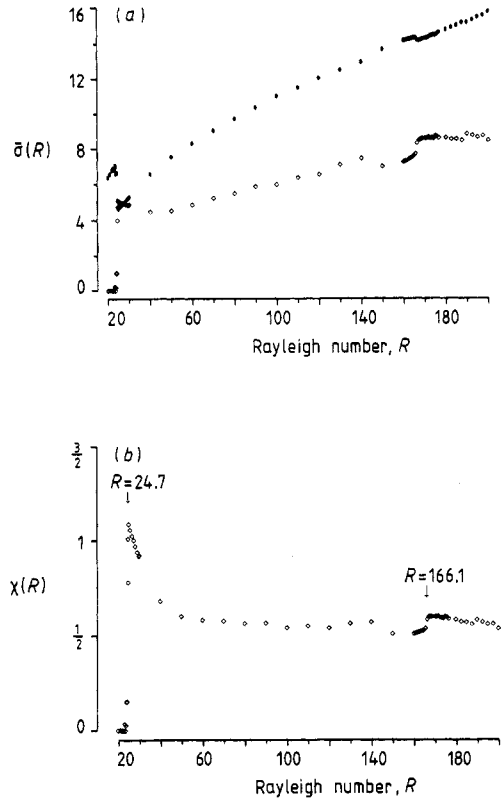

Figure 9. (*a*) $\bar{\sigma}(R)$ plotted against R and (*b*) $\chi(R)$ plotted against R for the Lorenz system. Averaging was performed over five random initial conditions, each of which was averaged for 1000 time units. Errors were maintained so χ is accurate to ± 0.01 throughout this range of R, though typically errors were an order of magnitude less than this figure. Note the almost discontinuous jumps in χ around $R = 24.6$ and 166.1. In (*a*) $\diamond$ plots $\bar{\sigma}_{\mathrm{Re}}$ and $\bullet$ plots $\bar{\sigma}_{\mathrm{Im}}$.

Changes in χ do not necessarily distinguish regular from chaotic motions. Rather, a change in χ indicates a change in the geometry of the attracting set (as illustrated, for example, by the distortion of the non-chaotic limit cycle of the Van der Pol oscillator). However, for the non-integrable systems that we have studied a sharp jump in χ seems to indicate the appearance of chaotic motion. The ease with which χ, as well as $\bar{\sigma}_{\mathrm{Re}}$ and $\bar{\sigma}_{\mathrm{Im}}$, can be obtained suggests that these numbers could provide a valuable diagnostic for charting regions of unknown dynamics in a large parameter space.

We conclude, however, with a word of caution. All the examples given in this section are dissipative systems. In the case of conservative Hamiltonian systems of two or more degrees of freedom, σ^2 does not always appear to be a very useful quantity. For example, in the case of the Hénon-Heiles Hamiltonian

$$H = \tfrac{1}{2}(p_1^2 + p_2^2 + q_1^2 + q_2^2) + q_1^2 q_2 - \tfrac{1}{3}q_2^3 \tag{4.9}$$

one may easily determine that σ^2 is a negative constant for all initial conditions. In cases such as this it may be necessary to go to higher traces to obtain the desired information. Alternatively, it is possible that we should try to calculate the persistence of strain using only the configuration space variables (the q_i above), i.e. project out

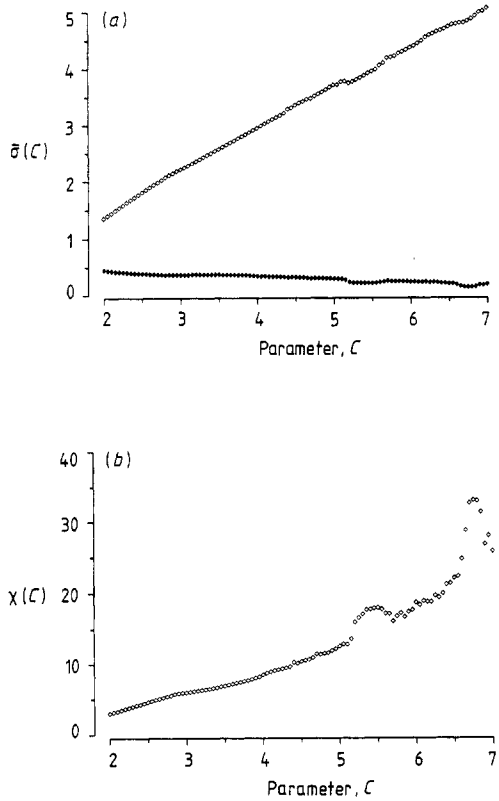

Figure 10. (*a*) $\bar{\sigma}(C)$ and (*b*) $\chi(C)$ for the Rössler attractor in the regime $2 \leqslant C \leqslant 7$. χ and $\bar{\sigma}$ are averaged over five random initial conditions. Errors were maintained so that χ is accurate to about ± 0.01. In (*a*) $\diamond$ plots $\bar{\sigma}_{\mathrm{Re}}$ and $\bullet$ plots $\bar{\sigma}_{\mathrm{Im}}$.

the momentum variables. The nature of σ^2 and χ for such Hamiltonians requires further investigation.

Acknowledgments

This work is supprted by ONR grant no N00014-85-K-0239. ED is supported in part by a Boris A Bakhmeteff fellowship. MT is an Alfred P Sloan research fellow. The authors thank M V Berry and B O'Shaughnessy for useful conversations.

References

Aref H 1983 *Ann. Rev. Fluid Mech.* **15** 345-89
Berry M V and Mackley M R 1977 *Phil. Trans. R. Soc.* **287** 1-16
Chaiken J, Chevray R, Tabor M and Tan Q M 1986 *Proc. R. Soc.* A **408** 165-74
Dombre T, Frisch U, Greene J M, Henon M, Mehr A and Soward A M 1986 *J. Fluid Mech.* **167** 353-91
Frank F C and Mackley M R 1976 *J. Polym. Sci.* A **2** 1121-31
Tabor M and de Gennes P G 1986 *Europhys. Lett.* **2** 519-22
Truesdell C 1954 *The Kinematics of Vorticity* (Bloomington: Indiana University Press)